Appl. Phys. B 59, 321–326 (1994)

Applied Physics B Lasers and Optics

Near-UV sub-Doppler spectroscopy on a metastable Mg beam by a frequency-doubled diode laser

N. Beverini, G. L. Genovesi, E. Maccioni, A. M. Messina, F. Strumia

Dipartimento di Fisica dell'Università di Pisa and I.N.F.M., Unità di Pisa, I-56126 Pisa, Italy
(Fax: +39-50/48 277, E-mail: BEVERINI@difi.unipi.it)

Received 15 November 1993/Accepted 25 March 1994

Abstract. Near-UV radiation is generated by doubling the frequency of a semiconductor laser in a nonlinear crystal. The crystal is contained in a resonant cavity in order to improve the conversion efficiency. The cavity increases the efficiency by about three orders of magnitude. This radiation has been used to perform spectroscopy of metastable magnesium in an atomic beam. We observed the $(3s3p)^3P-(3s3d)^3D$ transition multiplet, which is of interest for metrological applications. The isotopic shift between ^{24}Mg and ^{26}Mg was measured and new information on the hyperfine structure of ^{25}Mg was obtained. This radiation source is promising also in order to improve the Mg frequency standard.

PACS: 42.65, 32.00

The use of semiconductor lasers for spectroscopy is very attractive, especially when long-term, reliable operation of the laser source is a primary requirement. This is the case for metrological applications. Low-cost single-mode diode lasers, which can be easily tuned in frequency, are commercially available in the red and in the near-infrared between 750 nm and 850 nm. The use of these lasers for spectroscopical applications is described in detail in [1, 2]. Linewidths narrower than 1 MHz are easily obtained and a single laser can be tuned over a range larger than 20 nm. The technique of Second-Harmonic Generation (SHG) in a nonlinear crystal allows the extension of the use of semiconductor lasers to the blue and near-UV spectral regions.

In this paper we describe a laser source which produces a few hundreds μW of power at 383 nm, in the near UV. This frequency is obtained by SHG of a diode laser. We also discuss the application of this source to the spectroscopy of an atomic beam of metastable magnesium.

1 Second-harmonic generation in nonlinear crystals

When the type-I phase-matching condition can be accomplished and a Gaussian laser beam is focused into the center of the crystal, the SHG power $P_{2\omega}$ can be evaluated as a function of the incident power P_ω as:

$$P_{2\omega} = \frac{2\omega^2}{\pi n^3 \varepsilon_0 c^3} d_{\text{eff}}^2 P_\omega^2 l k_\omega \exp(-\alpha' l) h_m(B, \xi), \quad (1)$$

where d_{eff} is the nonlinear effective optical coefficient, n the refraction index, k_ω the wavenumber at the fundamental frequency, l the crystal length and $\alpha' = \alpha_\omega + \frac{1}{2}\alpha_{2\omega}$ its absorption coefficient. The function $h_m(B, \xi)$, where ξ is the focusing parameter of the laser beam and the parameter $B = \varrho(lk_\omega)^{1/2}/2$, proportional to the crystal double refraction angle ϱ, is given by Boyd and Kleinman [3]. They have demonstrated that $h_{mm}(B) \approx 0.714/B$ for $B > 2$, in conditions of optimum focusing. The formula is valid in the hypothesis of small conversion efficiency ($P_{2\omega} \ll P_\omega$).

The efficiency of direct SHG of a cw diode laser is limited by the low power of the available lasers. The technique of SHG in an external resonant cavity can be used to overcome this problem, as originally suggested by Ashkin et al. [4]. Very high conversion efficiency in the blue [5] has been obtained with this technique, using a $KNbO_3$ crystal. Unfortunately, $KNbO_3$ cannot be used at shorter wavelengths. The best choice in the near UV is the $LiIO_3$ (LIO) crystal. It can be tuned to type-I phase matching by angle tuning. At the wavelength of 383 nm the angle θ is about 45°. The non-linear coefficient $d_{\text{eff}} = d_{31} \sin(\theta + \varrho)$ is ≈ 2.9 pm/V, and its double refraction angle ϱ is 4.4°. Thus, a LIO crystal 15 mm in length has $B \approx 18$, $h_{mm} \approx 0.04$, and, according to (1), its optimized SHG efficiency $P_{2\omega}/P_\omega^2$ (neglecting the absorption factor) is expected to be of the order of 0.223×10^{-3} W^{-1}. Experimentally, we have obtained 0.157×10^{-3} W^{-1} from single-pass SHG (Fig. 1). It is worth to note that we have obtained this results by matching the diode lasers' ellip-

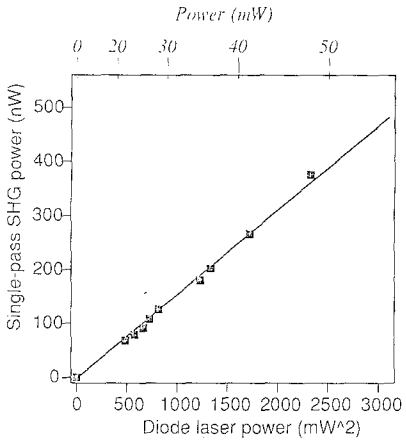

Fig. 1. UV power at 383 nm, obtained in a LIO crystal 15 mm long by single-pass SHG, as a function of the incident power

tical waist to the crystal asymmetry, so that the light beam was focused stronger in the direction of the non-critical crystal axis. In the opposite orientation the efficiency was lower more than 30%.

2 SHG experimental setup

The setup for laser SHG is shown in Fig. 2. We use a Spectra Diode laser, type SDL-5411-G1 as laser source. Its emission wavelength is 780 nm at 25° C, with 100 mW maximum output power. The laser chip is cooled down to a temperature of about −30° C by a Peltier module in order to reach the wavelength of 766 nm. In these conditions, the laser operates no more on single mode for output powers exceeding 85 mW. The whole system is kept in a vacuum chamber with an output window AR coated in order to achieve this temperature easily and to avoid water condensation. A home-made temperature controller stabilizes the temperature within 1 mK.

The LIO crystal is placed in a Fabry-Perot resonant cavity made by two spherical mirrors of 30 mm of curvature radius. The input mirror has a reflectivity $R_1 = 97.1\%$ at 766 nm. The output mirror is dichroic with a transmission $T_2 = 0.2\%$ at 766 nm and $T_2 = 88\%$ at 383 nm, and can be moved by a PZT to scan the length of the cavity. The laser light is focused to the center of the cavity through an AR coated lens with a focal length of 100 mm. Two optical isolators, with a whole isolation of about −75 dB and a total transmission of 72%, are inserted between the laser and the cavity, in order to avoid unwanted optical feedback. The whole system is held fixed on a solid and stable structure built on four steel rods.

The finesse of the cavity was measured to be greater than 80 (limited by the laser linewidth, which is about 15 MHz) and the free spectral range is about 1.25 GHz. A beam splitter transmitting about 0.94 is inserted between the optical isolator and the SHG cavity. Therefore, only about 56 mV are available at the input mirror. Only a fraction of this power can be coupled to the TEM_{00} resonant mode, because the laser beam cross section is elliptical. In fact, the measurement of the power reflected by the cavity shows that about 44% of the incoming power is reflected back at resonance. The reflected intensity is expected to be much smaller for a better laser beam cross section, because the input mirror reflectivity was selected to match the internal cavity losses (estimated to be about 3%). In conclusion, the power really injected into the cavity is about 32–36 mW. The power transmitted by the output mirror is 2 mW, corresponding to an intracavity circulating power of 1 W, and an enhancement of about 31. In these conditions, the maximum second-harmonic power from the cavity is about 200 μW; a result in good agreement with the expected intracavity SHG enhancement of about 1000, and with the single-pass SHG observed from the same crystal (about 0.2 μW for a beam intensity of 33 ≈ 36 mW).

The laser wavelength was locked to one of the cavity resonance modes by a feedback circuit that analyses the polarization of the radiation reflected by the cavity. This method, originally applied to laser frequency stabilization by Hänsch and Couillaud [6], exploits the 180° phase

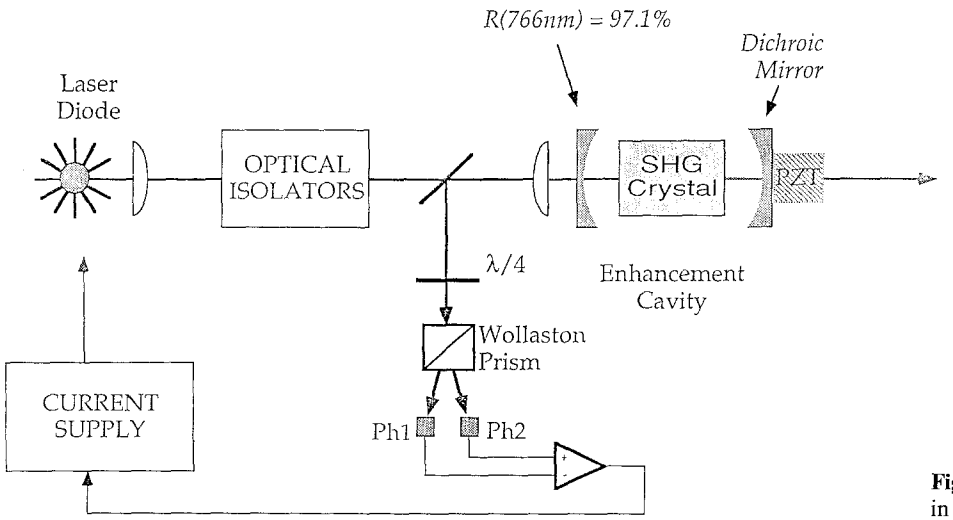

Fig. 2. Apparatus for SHG in an enhancement cavity

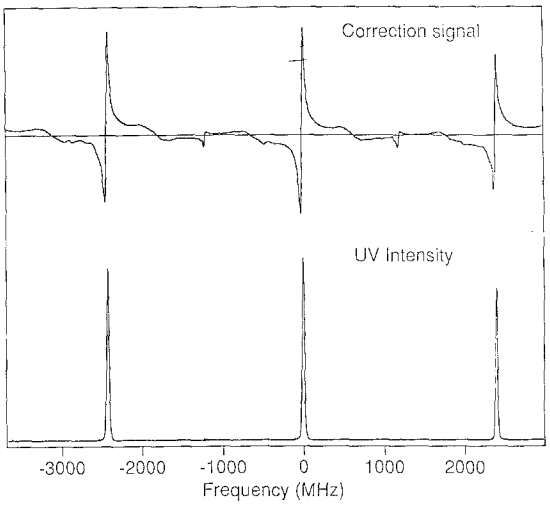

Fig. 3. Polarization of the radiation reflected from the SHG cavity, as observed through the ellipticity analyzer, while the diode-laser frequency in swept (*top*). SHG power transmitted by the cavity (*bottom*)

shift that the radiation reflected from a cavity exhibits, when the frequency is swept across the resonance. If the cavity contains a polarization discriminator, in our case a birefringent crystal, that forms an angle θ with the polarization vector of the incident wave, this phase shift can be detected analysing the polarization of the reflected wave. In fact, this wave is the result of the interference between the polarization component parallel to the intracavity polarizer, which is phase shifted with respect to the orthogonal component, which is reflected directly by the input mirror and is then insensitive to the resonance. As a result, the reflected wave shows a frequency-dependent ellipticity. A beam splitter samples the reflected wave and the two circular components are separated by a $\lambda/4$ plate and a Wollaston prism, and are detected by two photodiodes. A differential amplifier produces a dispersion-shaped resonance signal, that can be used as correction signal for electronic frequency stabilization. We have found that an efficient locking can be obtained also with a value of θ of the order of 5°. In these condition the loss of useful radiation for SHG is limited practically only to the insertion loss of the beam splitter. Figure 3 shows a typical recording of the reflected-wave polarization signal (Fig. 3a), together with the UV SHG (Fig. 3b), obtained by tuning the laser frequency. The capture range of the servo results to be ± 300 MHz. The bandwidth of the electronics is of the order of 1 kHz, which is the best compromise between short-time frequency noise of the locking system and its stability against large external perturbation (the system is quite sensitive especially to acoustic noises). In this condition the lock is usually maintained for times longer than one hour. The final linewidth of the frequency-doubled radiation is of the order of 25 MHz, since the locking system is too slow to affect the short-time stability of the laser.

The cavity resonance frequency can be scanned by a PZT glued to the input mirror, and the servo circuit is able to track continuously the SHG radiation over the whole PZT range (about 7 GHz in the UV).

3 Magnesium-beam spectroscopy

The Mg atom has a metastable triplet state $(3s3p)\ ^3P$ of high interest for metrological application [7, 8]. These levels are connected by three strong lines around 383 nm to the $(3s3d)\ ^3D$ level, which has a natural width of 27 MHz (Fig. 4). All the excited atoms return by spontaneous emission decay to the metastable triplet. As a consequence, these lines allow optical pumping between the metastable levels and laser cooling of the atoms in the $^3P_2$ level, through the $^3P_2$–$^3D_3$ component [8, 9]. These laser manipulations are very important in order to improve the performance of the Mg atomic frequency standard [10].

Natural magnesium is the mixture of three isotopes, with mass numbers 24 (abundance 78.70%), 25 (10.13%), and 26 (11.17%). Only the odd isotope has a nuclear spin ($I=5/2$) and thus presents a hyperfine structure.

It is useful for the applications to know the spectroscopical parameters of this transition. The isotopic shift was measured by Hallstadius [11] to be rather small; the 26–24 difference is 60 MHz and the 25–24 difference is 30 MHz. This is important for metastable optical pumping, because a single-frequency laser can pump, at the same time, different isotopes. However, the presence of a large hyperfine structure changes the situation in the case of the ^{25}Mg isotope. The hyperfine structure of the ^3P level has been measured with good resolution [12–13], while no experimental data exist for ^3D levels.

We have performed our measurements on a beam of metastable atomic magnesium, which is working since many years in our laboratory. The atoms exit from an

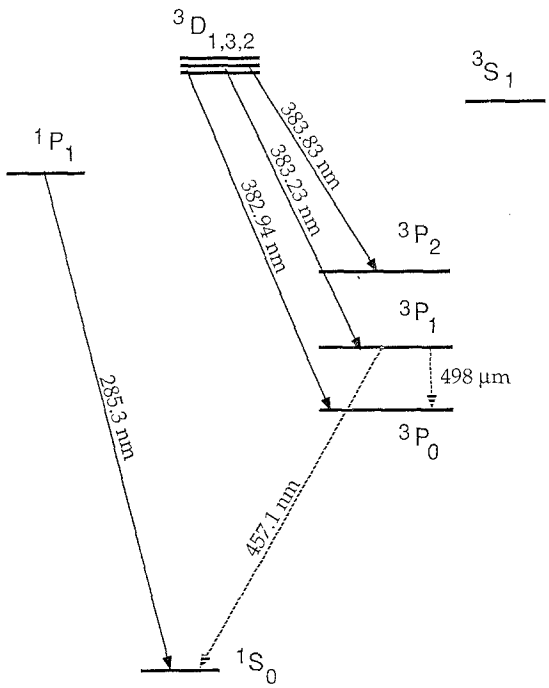

Fig. 4. Simplified level scheme of Mg. The magnetic dipole transition $^3P_0$–$^3P_1$ at 498 μm (602 GHz) is the reference transition for the Mg atomic clock

oven in a thermal effusive regime. An electronic self-sustained discharge excites the beam just in front of the hole with very high efficiency (≈30–40%). The collimation factor of the beam is of the order of 1:100.

3.1 Fine and hyperfine structure of the ^3P–^3D multiplet

We have sent the radiation produced by our frequency-doubling system in the direction orthogonal to the atomic beam, and we have detected the induced fluorescence by a photomultiplier (Fig. 5). A photodiode samples the intensity of the UV radiation in order to correct the intensity variation during the frequency scanning. The laser wavelength is measured with a lambda-meter interferometer and the frequency scanning is calibrated by a 300 MHz Fabry-Perot cavity.

We have tuned the laser frequency around the $^3P_0$–^3D, $^3P_1$–^3D, $^3P_2$–^3D multiplet at 382.93 nm, 383.23 nm, and 383.83 nm, respectively. The ^3D fine structure [14] is small enough to be contained in a single laser scanning. The experimental results are shown in Figs. 6–8. The fine structure frequencies fit the values given in [14]. The presence of ^{26}Mg can be deduced from

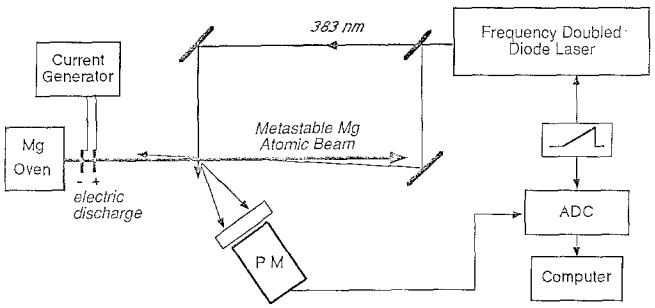

Fig. 5. Experimental apparatus for the spectroscopy of metastable Mg atoms. The 383 nm radiation is sent orthogonally to the beam, in order to obtain Doppler-free spectra. A second beam, nearly counterpropagating to the atomic beam, allows the measurement of the velocity distribution by the Doppler effect

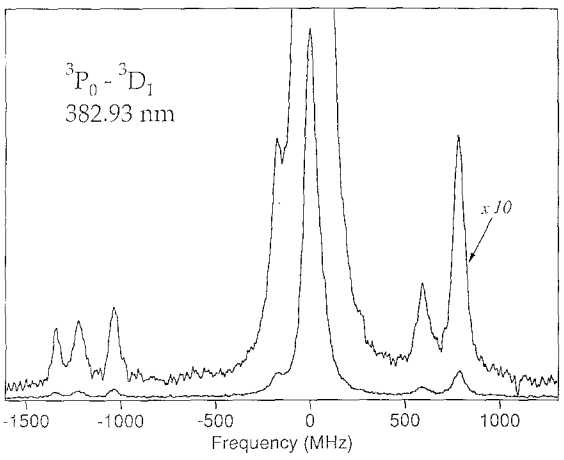

Fig. 6. $^3P_0$–^3D spectrum at 382.93 nm

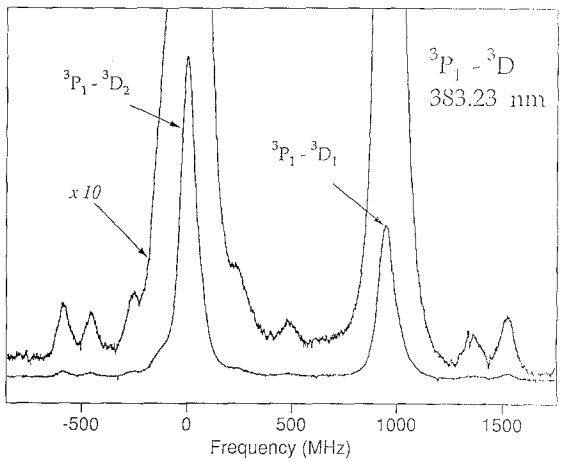

Fig. 7. $^3P_1$–^3D spectrum at 383.23 nm

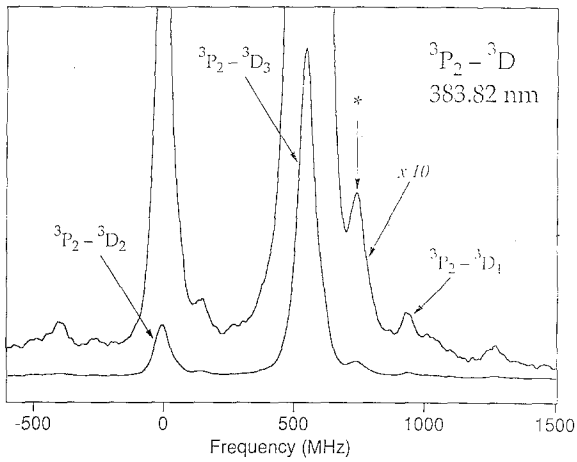

Fig. 8. $^3P_2$–^3D spectrum at 383.83 nm. The asterisk (*) shows the position of the ^{25}Mg $^3P_2$ ($F=9/2$)→^3D ($F=11/2$) component

Table 1. Isotope shifts ^{26}Mg–^{24}Mg observed in the present work, compared with previous results. All values are in MHz

	$^3P_0$–$^3D_1$	$^3P_1$–$^3D_2$	$^3P_2$–$^3D_2$	$^3P_2$–$^3D_3$
Hallstadius [11]	60*	60.6±3.0	58.2±3.6	
This work	65.0±3	61.3±6	62.5±4	67.6±3

* This value is given by the author as affected by a large error

the asymmetric deformation of the ^{24}Mg profile. We have extracted the relative shift of ^{26}Mg $^3P_0$–$^3D_1$, $^3P_1$–$^3D_2$, $^3P_2$–$^3D_2$, and $^3P_2$–$^3D_3$ transitions by analysis of the asymmetry of the lines. The intensity of these components is consistent with the isotopic abundances. The results are summarized in Table 1. The larger value found for the $^3P_2$–$^3D_3$ transition is probably due to the presence of a hyperfine component of ^{25}Mg, near the ^{24}Mg peak.

The hyperfine structure of ^{25}Mg is well evident. It is, however, very difficult to explain these spectra completely. In fact, the situation of the hfs of ^{25}Mg is quite peculiar. The fine structure of the ^3D multiplet is small, with a large contribution from the electronic quadrupole

term. At the same time the hfs interaction, caused by the $3s$ electron, remains approximately the same as in $(3s3p)$ ^3P metastable levels. As a result, the fine splitting and the hyperfine splitting are of the same order of magnitude, and the usual assumption that hyperfine interaction is small and can be treated as a perturbation with respect to fine structure breaks down entirely [15, 16]. In these conditions, levels with the same F, but different J, are mixed together, thus changing the frequency and the intensity of the transition components. A theoretical treatment of this situation can be found in Güttinger and Pauli [17]. This effect is particularly evident on the $^3P_0$–^3D transition (Fig. 6), where the perturbation theory would expect three components, due to $^3D_1$ splitting, with relative intensity 3:5:7. It should be noted that Hallstadius [11] was not able to obtain an accurate determination of the isotope shift of this particular transition because of "the presence of one or more interfering lines".

The presence of the large signal of ^{24}Mg, whose spectral profile cannot be known with enough accuracy, does not allow a complete interpretation of the spectra. We can however deduce some useful information. In the $^3P_2$–^3D transition (Fig. 8) the ^3D level with $J=3$, $F=11/2$ cannot be mixed with other levels. Then the component $^3P_2$, $F=9/2 \rightarrow {}^3D_3$ $F=11/2$ is not perturbed and can be identified by its intensity. Because the coupling of the $3d$ electron to the nuclear magnetic moment and to the nuclear electric quadrupole is completely negligible [16], we deduce a hfs a-factor for the $3s$ electron in the ^3D configuration of 380 MHz, in rough agreement with the value of 474 MHz reported by Lurio [12] for the ^3P configuration. We note that some hfs components of ^{25}Mg fall near the resonance frequency of ^{24}Mg, both for the $^3P_1$–^3D transition and the $^3P_2$–^3D transition. This fact can increase the efficiency of optical pumping of the metastable level in a beam of natural Mg and can explain, for example, the better efficiency obtained by $^3P_1$–$^3D_2$ pumping with respect to $^3P_1$–$^3D_1$ [9].

3.2 *Optical pumping of the metastable beam*

We have also tested the use of this SHG radiation for the optical pumping of the Mg atoms out of the $^3P_1$ metastable level. The measurements performed by using a dye

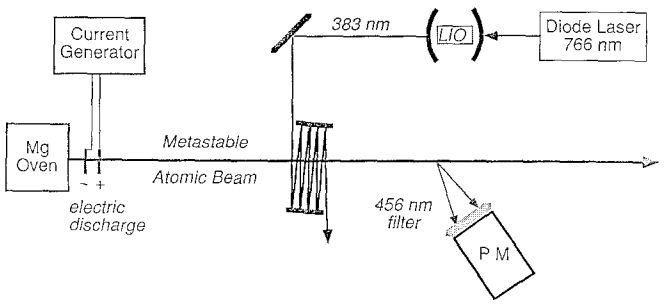

Fig. 9. Experimental apparatus for $^3P_1$ optical pumping by using the frequency-doubled laser diode

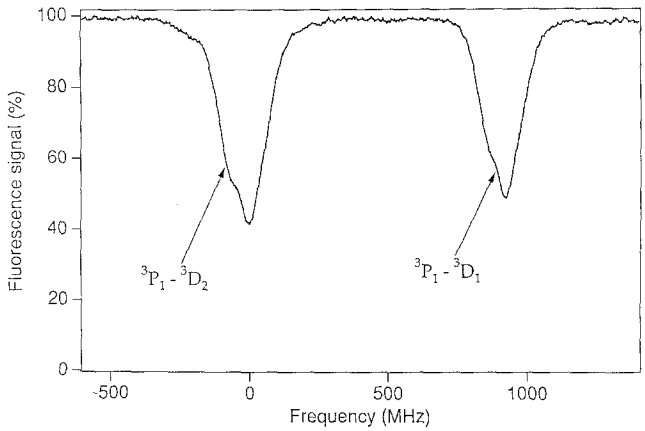

Fig. 10. Metastable beam fluorescence at 457 nm, when the beam is pumped by 383.23 nm radiation. The two minima coincide with the $^3P_1 \rightarrow {}^3D_1$ and $^3P_1 \rightarrow {}^3D_2$ transitions

laser [9] have demonstrated that a UV power of the order of 1 mW was necessary to obtain a good efficiency. We have used the multiple reflections in two dielectric mirrors, having a reflectivity exceeding 98%, to increase the pumping efficiency (Fig. 9). In Fig. 10 we show the signal recorded by a photomultiplier, that observes the fluorescence at 457 nm, due to the forbidden $^3P_1$–$^1S_0$ decay downstream the pumping region, while the diode laser is tuned around the $^3P_1$–^3D transition. The UV power incident on the beam was only of about 120 μW, due to the optical losses in the transmission of the light from the doubling crystal to the beam. We have observed a reduction in the detected fluorescence of 56%. At this level, the S/N ratio of the resonance signal in the Mg atomic clock, and consequently its stability, can be expected to increase by a factor larger than 5.

3.3 *Velocity distribution in the metastable $^3P_2$ level*

We were also able to observe the velocity distribution of the metastable atoms in the beam, by using our laser frequency doubling system. For this purpose, we have added a beam splitter to the apparatus used for the Mg spectroscopy, and we have observed also the fluorescence induced by the second laser beam, sent in the opposite direction to the atomic beam (Fig. 5). The laser is tuned around the $^3P_2$–^3D transition. Figure 11 shows a typical result, and demonstrates the deviation from a Maxwellian distribution, as a consequence of the loss of low-velocity atoms by collisions with the electrons in the excitation region [18]. The two narrow peaks are due to the fluorescence induced by the orthogonal laser beam. The velocity scale has been calculated with reference to the larger one, corresponding to the $^3P_2$–$^3D_3$ transition. The smaller peak, at about 600 MHz, corresponds to the $^3P_2$–$^3D_2$ transition, that has a probability lower by a factor 5.5.

This setup is particularly convenient for monitoring the velocity distribution in a laser cooling experiment of the atoms in the $^3P_2$ level [8].

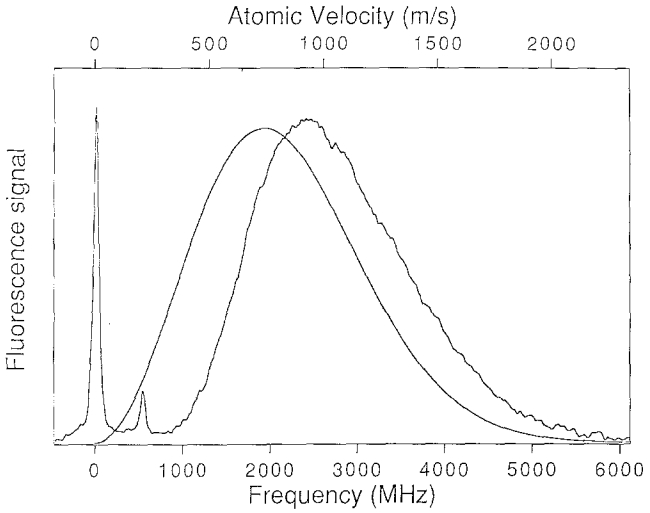

Fig. 11. Velocity distribution of the metastable $^3P_2$ atoms in the beam. The bottom scale shows the Doppler shift at 383 nm, relative to the $^3P_2 \rightarrow {}^3D_3$ transition. By comparison, the profile calculated from the Maxwellian distribution at the oven temperature is also shown (the presence of $^3P_2 \rightarrow {}^3D_2$ transition has been taken into account in the calculation

4 Conclusion

We have demonstrated that the frequency-doubled cw laser diode can be a useful tool for spectroscopy also in the region of the near UV, where powerful single-mode diode lasers at the corresponding IR wavelengths are commercially available. The power level which can be obtained is high enough for many spectroscopic and technological applications. The frequency-doubled diode laser cannot compete in power level with other cw laser sources available in the near UV, namely dye lasers and frequency-doubled Ti-Sapphire lasers, that can be more powerful by two or three orders of magnitude. However the reliability of these laser systems is not high enough to be implemented in metrological applications or other ones, in which the system must work continuously for a long time. In addition, these complex laser systems require a large frame ion laser as a pump, and, consequently, a special high-power electric line and a large cooling system. All these factors impose an installation and maintenance cost by far larger.

The power we have obtained in SHG can be still increased. The diode laser may be forced to work single-mode at the right frequency at its maximum power level by injection locking from a second narrow-band single-mode diode laser of lower power. The resulting narrowing of the laser linewidth would also increase the coupling efficiency. The use of an anamorphic prism for correcting the astigmatism of the laser beam may further increase the coupling efficiency. The efficiency of the optical isolators could also be increased. More powerful single-mode diode lasers up to almost 150 mW are expected to be commercially available in the near future. With the actual doubling efficiency, a 1 mW power level will be reached, with a power of about 100 mW at the input mirror. Finally, we hope that more efficient nonlinear crystals will be available in the future.

Acknowledgement. We are indebted to Mr. Mario Francesconi for his decisive contribution in the project and the construction of the different electronic systems.

References

1. C. Wieman, L. Hollberg: Rev. Sci. Instrum. **62**, 1 (1991)
2. K.B. MacAdam, A. Steinbach, C. Wieman: Am. J. Phys. **60**, 1098 (1992)
3. G.D. Boyd, D.A. Kleinman: J. Appl. Phys. **39**, 3597 (1968)
4. A. Ashkin, G.D. Boyd, J.M. Dziedzic: IEEE J. QE–**2**, 109 (1966)
5. G.J. Dixon, C.E. Tanner, C.E. Wieman: Opt. Lett. **14**, 731 (1989)
   A. Hemmerich, D.H. McIntyre, C. Zimmermann, T.W. Hänsch: Opt. Lett. **15**, 372 (1990)
   W.J. Kozlovsky, W. Lenth, E.E. Latta, A. Moser, G.L. Bona: Appl. Phys. Lett. **56**, 2291 (1990)
6. T.W. Hänsch, B. Couillaud: Opt. Commun. **35**, 441 (1980)
7. N. Beverini, F. Strumia: In *Laser Manipulation of Atoms and Ions,* ed. by E. Arimondo, W.D. Phillips, F. Strumia (North-Holland, Amsterdam 1992)
8. N. Beverini, E. Maccioni, F. Strumia: Laser Phys. (in press)
9. W.Q. Cai, N. Beverini, S. Del Tredici, J.V. Gomide, E. Maccioni, A.M. Messina, F. Strumia: SPIE Proc. **1726**, 212 (1992)
   N. Beverini, W.Q. Cai, S. Del Tredici, E. Maccioni, A.M. Messina, F. Strumia: Opt. Commun. (in press)
10. A. Godone, C. Novero: Metrologia **30**, 163 (1993)
11. L. Hallstadius: Z. Physik A **291**, 203 (1979)
12. A. Lurio: Phys. Rev. **126**, 1768 (1962)
13. A. Godone, E. Bava, G. Giusfredi: Z. Phys. A **318**, 131 (1984)
14. S. Isaksen, A. Andersen, T. Andersen, P.S. Ramanujan: J. Phys. B **12**, 893 (1979)
15. H.G. Kuhn: *Atomic Spectra* (Longmans, Green, London 1962)
16. H. Kopferman: *Nuclear Moments* (Academic, New York 1958)
17. P. Güttinger, W. Pauli: Z. Phys. **67**, 743 (1931)
18. G. Giusfredi, A. Godone, E. Bava, C. Novero: J. Appl. Phys. **63**, 1279 (1988)